

# Wafer-Wafer Bonding using Metal Silicides for High Temperature Applications

Eric Wu, Kirby Boone

SNF Mentors: Mahnaz Mansourpour, Usha Raghuram

External Mentor: J Provine

Stanford Nanofabrication Facility, Stanford University, Stanford, CA 94305

June 8, 2018

## Abstract

MEMS devices often require vacuum encapsulation in order to function. While there are several established techniques to form hermetic bonds for room-temperature operation, vacuum encapsulation for high-temperature extreme environment devices remains a challenge. In this project, we develop and characterize a wafer bonding process based on nickel silicidation that can potentially form a hermetic, electrically conductive seal for high-temperature MEMS and electronic devices, and for devices operating in challenging cesium vapor-containing ambients. We use nickel silicidation to bond both unpatterned and patterned substrates using the *evbond* in Stanford Nanofabrication Facility and study the dependence of bond quality on bonding temperature, force, and bond area. We characterize the quality of the bonds produced with qualitative testing methods like cleaving, dicing, and razor blade testing. We also quantitatively characterize the strength of the nickel silicide wafer bond using the double cantilever test. From these experiments, we conclude that nickel silicide wafer bonding is best performed at high bonding temperatures (450°C) and with high (~3340N) amounts of applied force.

## Introduction

Many MEMS devices, including pressure sensors, capacitive micromachined ultrasonic transducers (CMUTs), resonators, gyroscopes, and others, must be encapsulated in vacuum or in specific ambients to function properly. Wafer bonding is a common technique used to encapsulate MEMS devices, in which a lid wafer is bonded over a wafer containing MEMS devices, sealing the devices in their required operating environment. Although there are many established processes for wafer bonding for encapsulating MEMS devices [1], few of these techniques can be applied to packaging high temperature devices. For example, MEMS thermionic energy converters operate at temperatures greater than 1000°C in an ultra-corrosive cesium vapor environment. Here, we present and characterize wafer bonding by nickel silicidation. Nickel silicide wafer bonding potentially offers substantial advantages over more conventional bonding methods for extreme-environment MEMS and electronic devices, namely (1) the bond can be formed at moderate (<500°C) temperatures but can survive much higher temperatures without melting or otherwise reacting; and (2) the bond is likely to survive highly corrosive environments like cesium vapor. The process uses standard deposition, metallization, and patterning steps, and the bond itself can be made with a standard wafer bonding tool, making it feasible to integrate with MEMS fabrication flows.

## Review of standard wafer bonding techniques for MEMS

Several standard, well-established techniques for wafer bonding have been developed for MEMS applications, including anodic bonding, eutectic bonding, solder bonding, and direct bonding, and are briefly introduced [1].

Anodic bonding is a commonly-used MEMS packaging technique for bonding glass and silicon wafers. To perform anodic bonding, Pyrex and silicon wafers are pressed together with force at an elevated temperature (180-500°C) and a voltage is applied between the glass and silicon. The bonding process relies on an electrochemical process involving the motion of sodium ions and oxygen ions in the glass, and thus the process requires that a glass wafer containing a high concentration of alkali metals is used. Although anodic bonding is an established technique for MEMS vacuum packaging, it is unsuitable for specific applications like MEMS thermionic converters, as cesium vapor is known to attack SiO<sub>2</sub> catastrophically at high temperatures. Anodic bonding is commonly performed in the SNF using the *evbond* with the quartz pressure plate.

Eutectic and solder bonding are a related set of bonding techniques that rely on an intermediate metal layer to form the bond. In a eutectic bond, the intermediate bonding material mixes with another material to form an eutectic mixture that has a lower melting point than either of the two bulk materials, allowing bonds to be made at lower temperatures and reducing packaging stress due to CTE mismatch. Typical materials systems for forming eutectic bonds are Au-In, Al-Ge, and Au-Si. The process is usually performed in a wafer bonder by applying heat and pressure. For solder bonding, a solder intermediate layer (typically a low melting point mixture of metals) is heated and reflowed between the substrates to be bonded. Although eutectic and solder bonding are commonly used for fabricating commercial MEMS devices, they are both likely unsuitable for ultra-high temperature applications, as the bonding layers may melt or reflow at operating temperature, leading to failure of the device. Both eutectic and solder bonding can be performed in the SNF using the *evbond*.

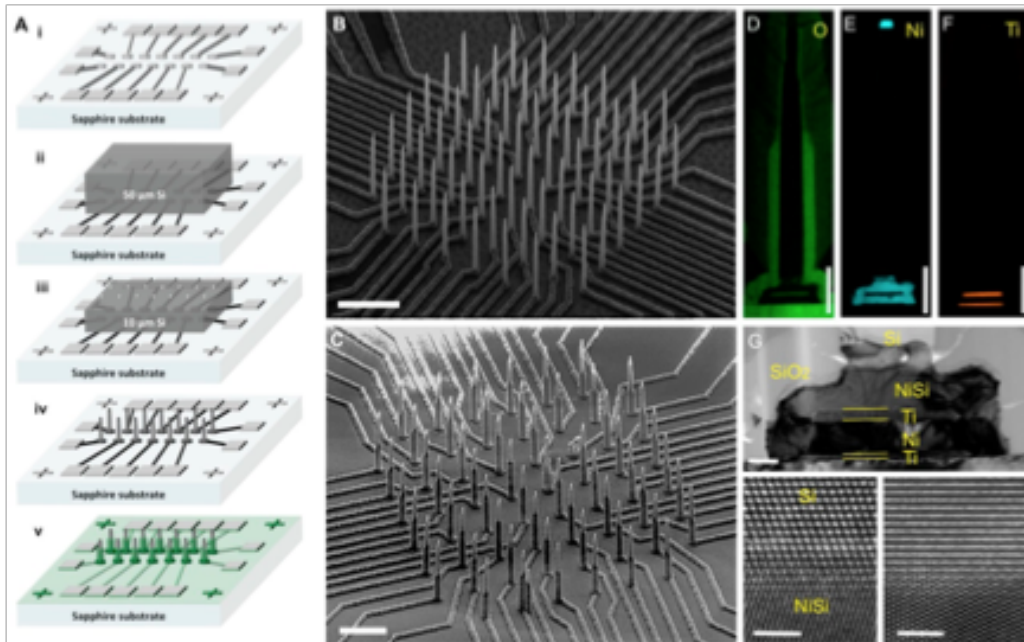
Direct bonding is a process in which wafers are bonded together without any intermediate layer. In a direct bonding process, two ultra-clean, reactive surfaces are pressed together at high temperature to form a bond. For successful bonding, the wafers, typically silicon, need to be particle-free and ultra-flat, and the surfaces of the wafers must be chemically

active. Because this process requires ultra-high temperatures on the order of 1000°C, direct bonding cannot be performed in the SNF using the *evbond* tool.

### Nickel silicide bonding: advantages and literature review

Nickel silicide wafer bonding has previously been demonstrated for fabrication of bonded wafer pairs and for heterogeneous integration. Xiao, *et al.* [2] demonstrated successful bonding of crystalline silicon pairs with a nickel silicide interface formed by annealing at 440°C and showed that the interface forms an ohmic contact. They confirmed using Auger spectroscopy and x-ray diffraction that the bonding interface indeed consisted of nickel silicide, and that NiSi is the dominant phase. Liu, *et al.* [3] used a nickel silicide wafer bonding process to fabricate high-aspect ratio crystalline silicon pillar electrodes on a sapphire substrate for neural probe arrays (Figure 1a). Dai, *et al.* [4] used a similar nickel silicide bonding technique for integration of III-V InGaAs FinFET transistors onto silicon substrates (Figure 1b)

(a)



(b)

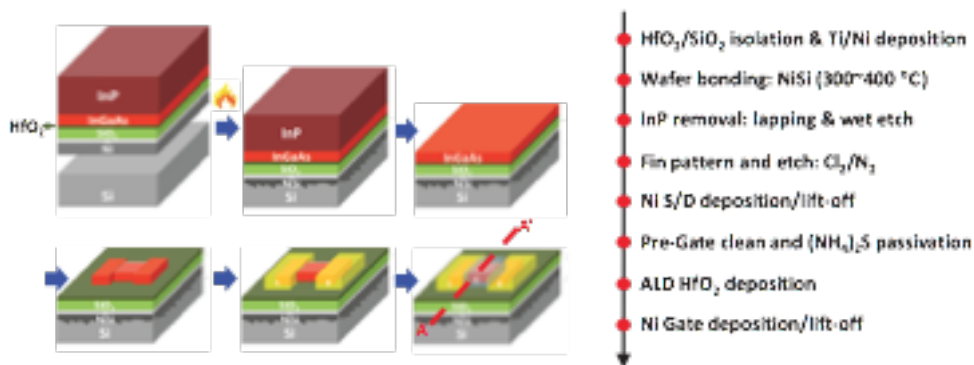


Figure 1: Examples of nickel silicide bonding for heterogeneous integration. (a) Taken from Liu *et al.* [3]. Tall, high aspect ratio crystalline silicon neural probes are fabricated on a sapphire insulating substrate by bonding a silicon layer onto conducting pads with nickel silicidation, and using e-beam lithography and etching to produce pillars. (b) Taken from Xiao *et al.* [2]. InGaAs III-V FinFET transistors on a silicon substrate are fabricated by patterning an InGaAs layer bonded onto a silicon wafer with nickel silicidation.

Nickel silicide and other metal silicide bonding techniques offer some advantages over standard wafer bonding techniques. In particular, the wafer bond can be formed by reacting the metal and silicon at moderate temperatures (potentially as low as 280°C for nickel), to produce a silicide that melts at much higher temperatures (up to 993°C for NiSi, and up to 1289°C for NiSi<sub>2</sub>). Silicide wafer bonding potentially enables processing and packaging of ultra-high temperature MEMS and electronic devices with conventional wafer bonding tools without compromising device performance. In addition, because nickel silicide and other metal silicides are conducting, the bonds themselves could be used as vertical feedthroughs and electrical interconnects in MEMS structures.

MEMS thermionic energy converters are an example of a device that could potentially benefit from the unique properties of a nickel silicide wafer bond (Figure 2). A thermionic energy converter is a two-terminal device that operates as an electronic heat engine. In a thermionic energy converter, thermally excited electrons are emitted from a high temperature cathode, travel across a vacuum gap, and are then collected at a higher energy level on the lower temperature anode. The operating temperatures of a thermionic energy converter are very high, with the cathode in the neighborhood of 1200°C and the anode in the neighborhood of 500°C. In order for the device to function, the bond must hold vacuum at the anode operating temperature. Furthermore, to enable straightforward electrical interconnection to the hot cathode, the bond ideally should be electrically conductive. Finally, since cesium vapor is typically used to lower the work functions of the cathode and anode for better device performance, the bond should be resistant to cesium vapor attack. Assembling thermionic energy converters with nickel silicide wafer bonds potentially satisfies all of these requirements, as nickel silicides melt at well above the anode operating temperature, are known to be electrically conductive, and are likely resistant to cesium attack (both bulk Ni and Si are known to be compatible with cesium) [5].

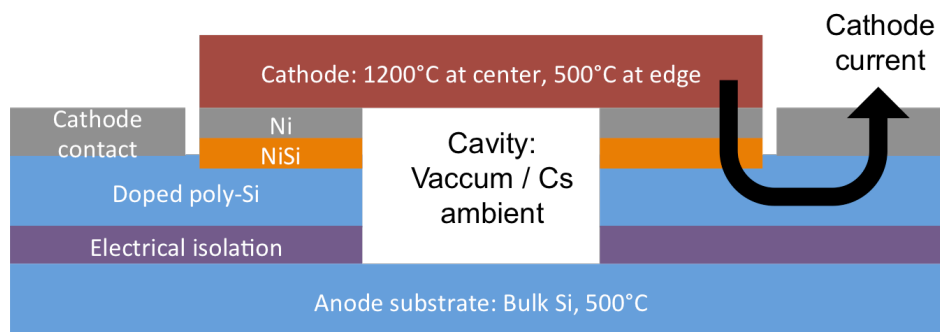


Figure 2. Cartoon schematic showing the possible application of nickel silicide wafer bonding for microfabrication of MEMS thermionic energy converters. The nickel silicide serves as a vacuum seal at the operating temperature of the device (500°C), and also serves as a vertical interconnect for electrically contacting the cathode.



## **EVBond primer, wafer bonding process variables, and design of experiments**

The *evbond* is a wafer bonder capable of doing eutectic, solder, and anodic bonding, and can be used to bond both 4-inch wafers and pieces. Because bonding can be done in a vacuum ambient, the tool can be used for MEMS vacuum packaging. The *evbond* setup in the SNF consists of a Megasonic cleaner and an EVG501 bonder. The Megasonic cleaner resembles a spin-coater and uses jets of water to remove particles from the surfaces of the wafers before bonding. The bonder consists of a bonding chuck and a pressure plate contained in a vacuum chamber. The bonding process can be summarized as follows:

1. Remove particles from wafers with the Megasonic cleaner
2. Load the wafers onto the bonding chuck and put bonding chuck into the bonder. Flags (small removable metal tabs) are used to separate the wafers.
3. Bond. The bonder pumps down, heats the chuck to the user-specified temperature (up to 500°C), removes the flags, and applies a user-specified force to squeeze the two wafers together. The tool maintains the specified temperature and force for a user-specified time interval. If doing anodic bonding, the tool also applies a user-specified voltage between the two wafers.



Figure 3. EVbond tool in the SNF, image taken from the SNF wiki. The tool on the left is the Megasonic cleaner, and the tool on the right is the bonder.

As with most bonding processes, the critical process parameters for nickel silicide wafer bonding are bonding force or pressure, bonding temperature, bonding surface area, and bonding time. For this project, we fixed bonding time at 40 minutes and focused on determining the dependence of bond quality on area, temperature, and force/pressure. To determine the relationship between bonding quality and bond area, we varied the pattern for the Ni bonding layer from blanket-coated wafers to arrays of 1cm x 1cm rings with fill factors of 10%, 25%, 50%, and 75% (Examples of the ring patterns are shown in Figure A1). We studied the dependence of the bond on temperature by bonding wafers at 300°C, 350°C, and 450°C. Finally, we characterized the dependence of bond quality on bonding force/pressure by scaling force to maintain a constant bonding pressure (decrease force proportionally with the decrease in Ni area), and then by bonding wafers with varying Ni areas at the maximum tool force of

3340N. The set of experimental parameters is summarized in Table 1, and the full set of experiments and their results are provided in Appendix D.

Table 1: Design of Experiments – primary variables tested were temperature and fill factor.

Temperature	Force	Bonding ring fill factor
300°C	3340 N	10%
350°C	1660 N	25%
450°C	1120 N	50%
	540 N	75%
	525 N	Unpatterned

### Process flow description

In brief, our process consisted of bonding unpatterned polysilicon-coated silicon wafers to patterned or unpatterned Ni-coated wafers. All substrates were new 4-inch K-prime silicon wafers purchased from the SNF stockroom, and were cleaned using a standard piranha (9:1 sulfuric acid:hydrogen peroxide) bath for 20 minutes before being processed.

Undoped polysilicon-coated wafers were fabricated with low pressure chemical vapor deposition (LPCVD) at 620°C on blank wafers, using a silane precursor. Deposition time was fixed at 1 hour and 55 minutes, with an estimated thickness of 1-2  $\mu\text{m}$ . After deposition, polysilicon wafers were stored until needed for bonding. The unpatterned nickel wafers were fabricated by sputtering a 10 nm titanium (Ti) adhesion layer/diffusion barrier followed by a 200 nm Ni bonding layer in the Lesker sputter. After sputter deposition, wafers were stored until needed for bonding.

Patterned nickel wafers were fabricated using an evaporation and liftoff process. Wafers were first singed and coated with hexamethyldisilazane (HMDS) in the YES oven at 150°C. A thin LOL2000 liftoff underlayer was spun on at the *headway2* manual coater, and the wafers were then baked in the *white-oven* for an hour at 180°C. Following that, the wafers were spin coated with 1.6  $\mu\text{m}$  of Shipley 3612 resist and pre-baked using the *svgcoat* automated coater track, then exposed using the Heidelberg MLA150 maskless exposure tool. The exposed pattern was developed using the *svgdev* automated developer track, baked once more at 90°C for 1 minute. Metal deposition was performed in the AJA evaporator. A 10 nm layer of Ti was first deposited at a 0.5  $\text{\AA}/\text{s}$  deposition rate as a sticking layer and to prevent Ni from diffusing back into the Si wafer instead of the polysilicon opposite wafer. A second layer of 150 nm of Ni was deposited at 0.5  $\text{\AA}/\text{s}$  after a ten minute cooling period inside the evaporation chamber. Metal liftoff was performed in acetone without agitation, and the wafers were left to soak in Microposit Remover 1165 overnight. A final isopropanol soak and rinse was used to remove any remaining chemical residue. Wafers were then stored until needed for bonding.

With the exception of one initial bonding trial, all wafers were chemically cleaned immediately before bonding. The nickel-coated wafers were cleaned by immersing in a mixture of 5:1 water:29% ammonium hydroxide for 5 minutes, based on the cleaning protocol taken from [3]. This clean was done to strip the surface nickel oxide. The native oxide of the polysilicon-coated wafers was stripped with a 1 minute dip in 50:1 HF. Wafers were loaded into the *evbond* and bonded as soon as possible after cleaning (typically within 30 minutes of completing the clean).

Bonding process conditions in the *evbond* (temperature, force/pressure) were varied according to the discussion above. After bonding, the samples were stored until they were ready to be subjected to the razor blade test or put through the wafer saw. Successfully bonded Ni ring samples were diced into 2 cm squares using the DISCO DAD3240 wafer saw to evaluate the extent and qualitative quality of bonding.

Cartoons illustrating the process are shown in Figure 4, and complete runsheets with the specific times, process parameters, and programs are attached in Appendix A to this report.

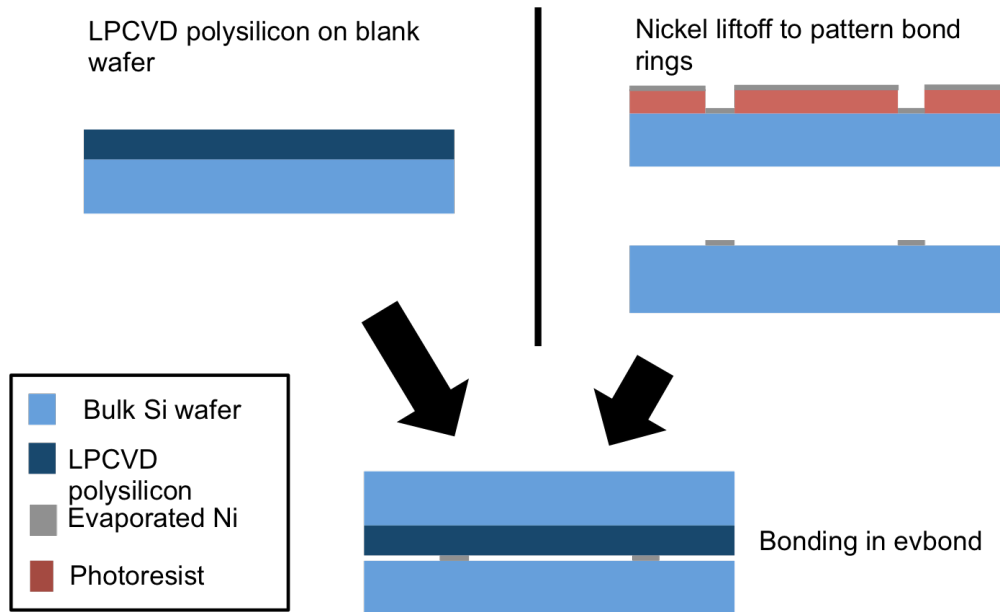


Figure 4. Cross-section cartoon showing fabrication process for patterned bonded structures. The polysilicon layer is fabricated by blanket-depositing LPCVD polysilicon on a blank silicon wafer. The nickel is patterned with a liftoff process. The wafer pair is then bonded in the *evbond*.

### SEM Imaging of Bonding Interface

We imaged the bonding interface using SEM to characterize the bonding interface and to help confirm that the bond is indeed the result of nickel silicide formation. Images were taken by cleaving a bonded wafer, mounting it on a vertical SEM mount, and imaging the bonding interface. While no spectroscopy techniques were used to explicitly confirm the materials composition of the bond, the thicknesses and appearances of the imaged films are very close to what we expect, suggesting that the bond is due to formation of nickel silicide. The SEM micrographs are shown in Figure 5.

(a)

(b)

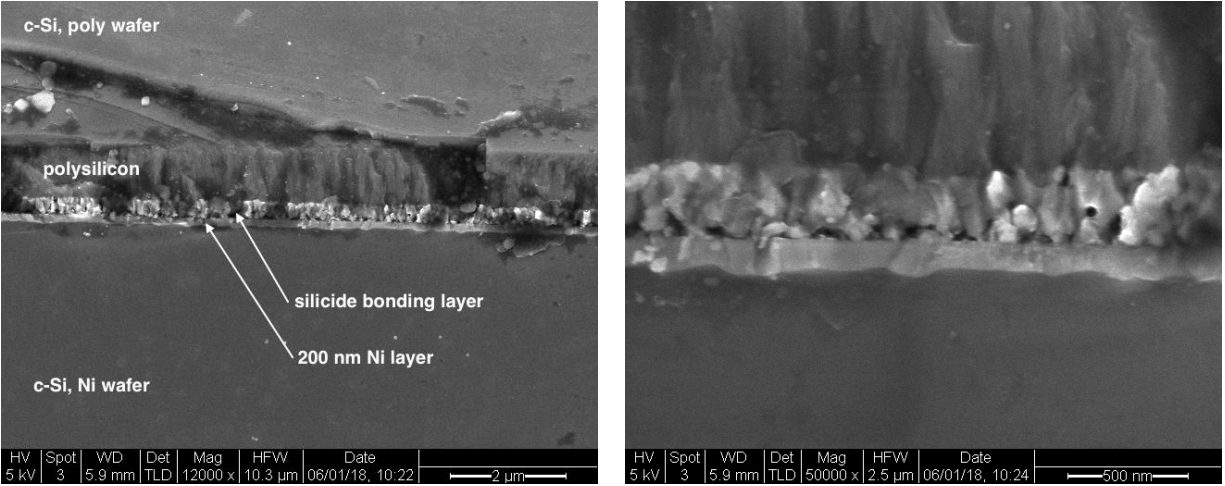


Figure 5. (a) Cross-sectional SEM image showing all layers of the bonding stack, with the layers annotated. The polysilicon-coated silicon wafer is at the top, with the frontside surface of that wafer facing down. The Ni-coated wafer is at the bottom, with the frontside surface of that wafer facing up. The nickel silicide forms at the interface. (b) Higher magnification SEM image of the nickel silicide bonding region. The rough light-colored region is the nickel silicide formed by the diffusion of Ni into polysilicon. The smoother light-colored region is either unreacted Ni, or nickel silicide formed by the diffusion of Ni into the crystalline silicon substrate.

A simplistic calculation of how deep the nickel may have diffused into the polysilicon layer to form NiSi can be approximated by Eqn. 1 below which assumes an unlimited source of diffusing material,

$$\frac{c(x,t) - c_0}{c_s - c_0} = 1 - \operatorname{erf}\left(\frac{x}{2\sqrt{D \cdot t}}\right) \text{ fraction/cm}^3 \quad \text{Eqn. 1}$$

where  $c_0$  is the original concentration in the surface,  $c_s$  is the constant surface concentration,  $D$  is the diffusivity of the species being calculated,  $x$  is position, and  $t$  is time. This equation takes the activity of the species as ideal, which is obviously not valid in the event of the chemical reaction producing NiSi as the bonding layer, but it gives a useful baseline for comparing against experimental observations. While perhaps not valid in the range of 450°C, the diffusivity of Ni in Si as referenced from Weber is  $D_{Ni,Si} = 2 \times 10^{-3} \exp\left(-\frac{0.47 \text{ eV}}{k_B T}\right) \text{ cm}^2/\text{s}$ , resulting in approximately  $D_{Ni,Si} = 1.22 \times 10^{-6} \text{ cm}^2/\text{s}$  at 450°C [5]. Plugging in a time of 40 minutes bonding time, Eqn. 1 indicates that a 10% concentration of Ni can be found at a depth of a little more than 1.25 μm into the polysilicon. Based on the SEM examination, the Ni clearly did not diffuse that deep into the polySi for a variety of potential reasons such as lower temperature inhibiting diffusivity and the silicide reaction impeding transport just as a passivating oxide layer might.

### Bonding surface roughness

Prior to the initial proof of concept test, the unpatterned Ni and polysilicon-coated wafers were examined using the Sensofar S-neox optical profilometer to estimate the surface roughness. While attempting to measure the roughness on the blanket coated wafers discovered that if the tool does not have sufficient surface contrast, artifacts in the tool programming produce the impression of a striated surface as seen in Appendix C. Therefore, our best estimate of the surface roughness RMS of the polysilicon coated wafer is less than 4

nm. S-neox analysis on patterned wafers did not produce this striation effect, and the surface of the evaporated Ni layer was determined to have a surface roughness RMS value of about 2 nm.

### **Pre-bond cleaning**

As part of our initial efforts to characterize the nickel silicide wafer bond, we attempted to bond unpatterned nickel and polysilicon-coated wafers without cleaning. These wafers were fabricated in a similar manner to others that successfully bonded; however, they were not chemically cleaned prior to bonding (no HF dip for the polysilicon-coated wafer, no ammonium hydroxide clean for the nickel-coated wafer). The wafers were bonded at 450°C for 40 minutes under 3340N, but separated immediately upon removal from the bonding chuck. Subsequently, we chemically cleaned and successfully bonded identical wafers using the same process parameters, demonstrating the necessity of chemically cleaning the wafers prior to bonding (especially the HF SiO<sub>2</sub> strip). All bonding attempts except for this initial attempt made use of the chemical cleaning process.

### **Qualitative characterization by cleaving, dicing, shattering, and razor blade**

To qualitatively assess the effects of bonding temperature, force, pressure, and area on the bond quality, we characterized the bonded wafers by cleaving, dicing, and shattering the bonded pairs, and then using a razor blade to attempt to separate the resulting pieces.

Cleaving, dicing, and shattering bonded wafer pairs are quick methods for qualitatively testing for bonding strength. These methods for singulating the wafer are very violent, and apply a tremendous amount of stress to the bonding interface. Successfully bonded wafers will remain bonded together through these processes, while poorly bonded wafers will fully or partially separate.

The razor blade test is a simple qualitative method for evaluating bond quality for bonded wafers or pieces. To perform the razor blade test, one tries to manually separate the bonded wafers or pieces by sticking the sharp edge of a razor blade into the bonding interface. Poorly bonded samples will separate easily and cleanly (the two sides will pop apart), while well-bonded wafers or pieces will break or chip rather than separate cleanly. Extreme caution must be taken to avoid accidentally cutting the tester's hands.

We recorded the results of these qualitative tests and assigned numerical scores to the results to help visualize trends in bond quality. A score of 0 corresponds to a poor quality bond or no bond at all, and was assigned to samples that separated completely immediately after bonding or during dicing/cleaving/shattering. A score of 1 corresponds to moderate bond quality and was assigned to samples that survived dicing/cleaving/shattering and showed some signs of bonding when separated with a razor blade. A score of 2 corresponds to good bond quality and was assigned to samples that survived dicing/cleaving/shattering and could not be separated during the razor blade test. Examples showing how bond quality was determined are given in Figure 6, and the full results table is appended to the end of this report as an appendix.

**(a)**

**(b)**

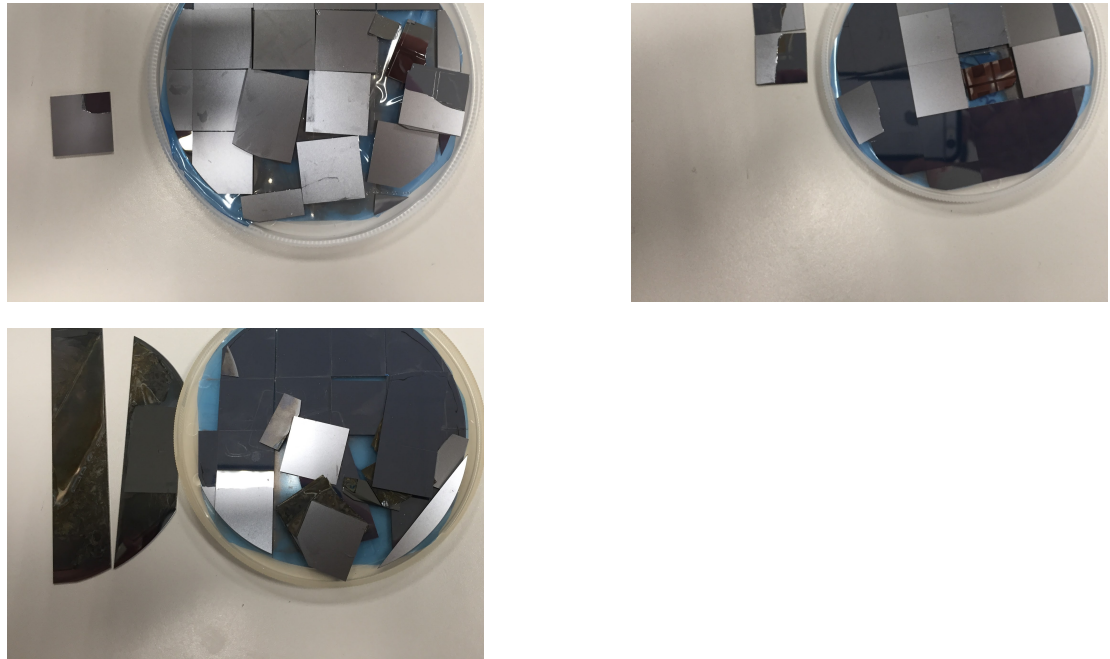


Figure 6. Examples of different quality wafer bonds after dicing and razor blade testing. (a) Good-quality wafer bond, assigned a score of 2. Pieces generally stayed together during dicing, and the resulting pieces were very difficult to separate without breaking using the razor blade test. (b) Moderate-quality wafer bond, assigned a score of 1. Some pieces remained together while dicing, while the surviving pieces could be separated with a razor blade with some signs of bonding. (c) Low quality wafer bond. All of the pieces separated during the dicing process.

The dependences of qualitative bonding quality factor on the input variables bonding temperature, bonding pressure/force, and bonding area are plotted in Figure 7. From these plots, it is clear that temperature is a critical process parameter, as results tended to be much better for bonds performed at 450°C than for bonds performed at lower temperatures. Bonding force is also an important process parameter, with high forces producing better results than low forces. The bond quality has little to no dependence on the bond pressure, calculated by normalizing the bonding force by the expected bonding area, suggesting that the bonding force should remain at a constant high value even as the bonding area is decreased. One potential explanation for this dependence on total force but not pressure is that a large force applied by the bonding chuck is needed to account for the curvature of the wafers. Bonding quality increased strongly with increasing total bond area, but did not have as strong a dependence on the width of the bonding rings themselves, suggesting that narrow bonding rings are feasible with this bonding technique. While it is clear that higher bonding forces and areas lead to better quality bonds, because of the design of experiments chosen for this project, it is difficult to determine whether total force or area is the dominant contributor. A few additional experiments with samples with low surface area bonded at high force and samples with high surface area bonded at low force should help to determine this.

(a)

(b)

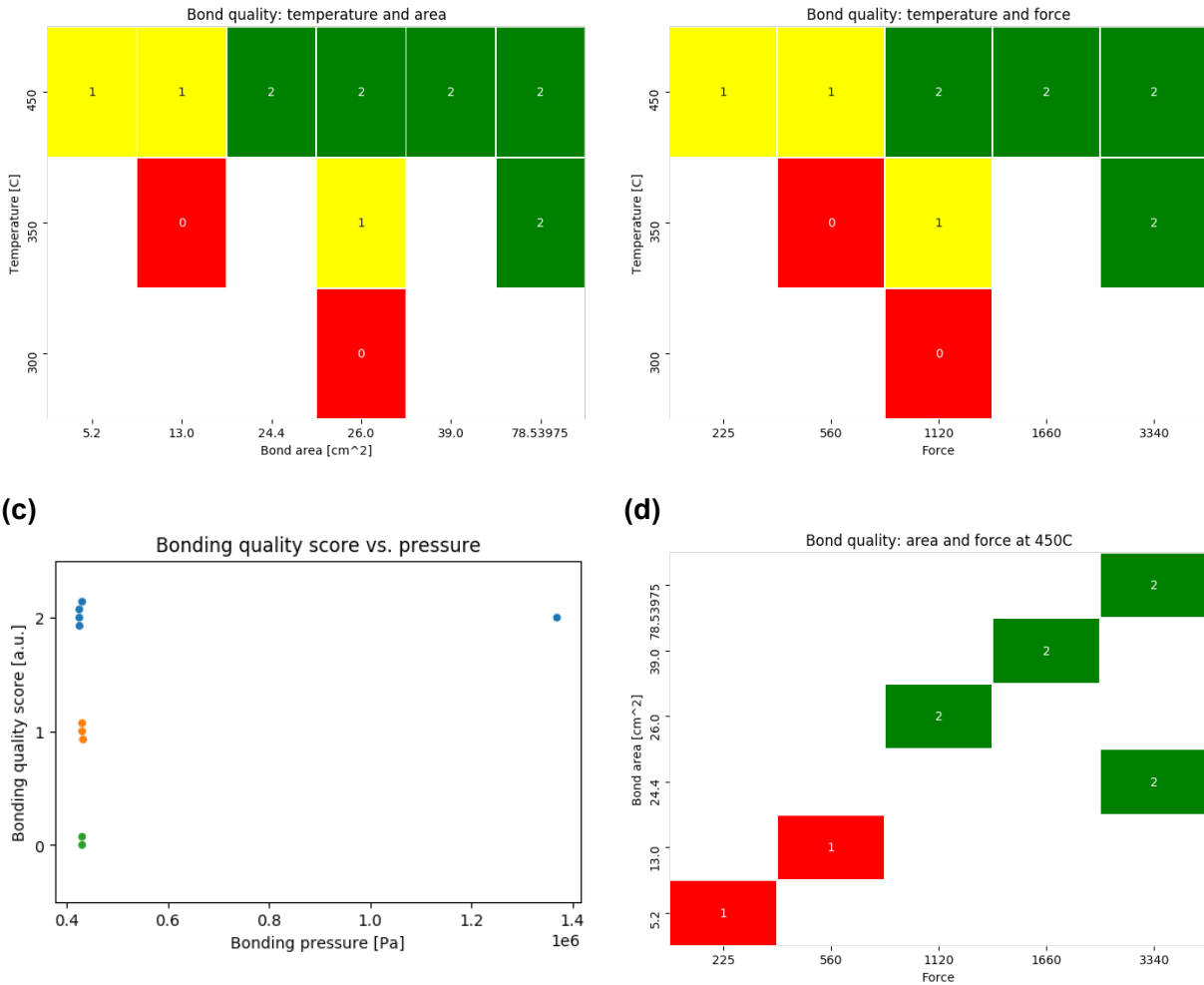


Figure 7. Qualitative bonding score plotted against bonding experimental variables. (a) Bond quality improves with higher bonding temperature and increased bonding area. (b) Bond quality improves with higher bonding temperature and higher bonding force. (c) Bonding quality does not depend on the pressure, defined as the bonding force divided by the patterned bonding area. (d) Bond quality as a function of area and force, for bonds performed at 450°C only. It is possible that bonding area and force are confounding variables in determining bond quality. Additional experiments to fill out the corners (large-area samples bonded at low force and low-area samples bonded at high force) would help definitively separate the effects of bonding force and area.

- Based on the above qualitative results for bonding quality as a function of temperature, force, and bonding area, we can make the following suggestions:
1. Bond at the highest temperature compatible with the samples and process being used. 450°C is sufficiently high for a good quality nickel silicide bond.
  2. Use the highest amount of bonding force that is compatible with the samples and process being used. While it may be tempting to scale down the bonding force as the bonding area is decreased, bonds performed at lower forces were generally worse than bonds performed at higher forces.

**Other qualitative observations**

We generally observed better bonding at the center of our wafers than at the edges. Pieces located near the edge of the bonded pair are much more likely to separate during cleaving or dicing than pieces located near the center of the wafer. This could be due to a variety of reasons, including but not limited to wafer curvature, particles and scuff marks from handling the wafers at the edges with tweezers, metal stringers at the edges that persisted after liftoff, and the distribution of force applied by the pressure plate of the bonder. Because of this, we suggest placing critical devices at the center of the wafer.

### Double Cantilever Beam Test

Two secondary Ni bonded wafers were prepared at 450°C and 350°C for 40 minutes at maximum *evbond* tool force (3340 N) with a special design for Double Cantilever Beam (DCB) testing. The design pattern with dicing lanes is below in Figure 8. After bonding and dicing, these were used as test sample beams with 5 cm of bonded material in the center and approximately 1.5 cm of unbonded “pre-crack” areas at each end.

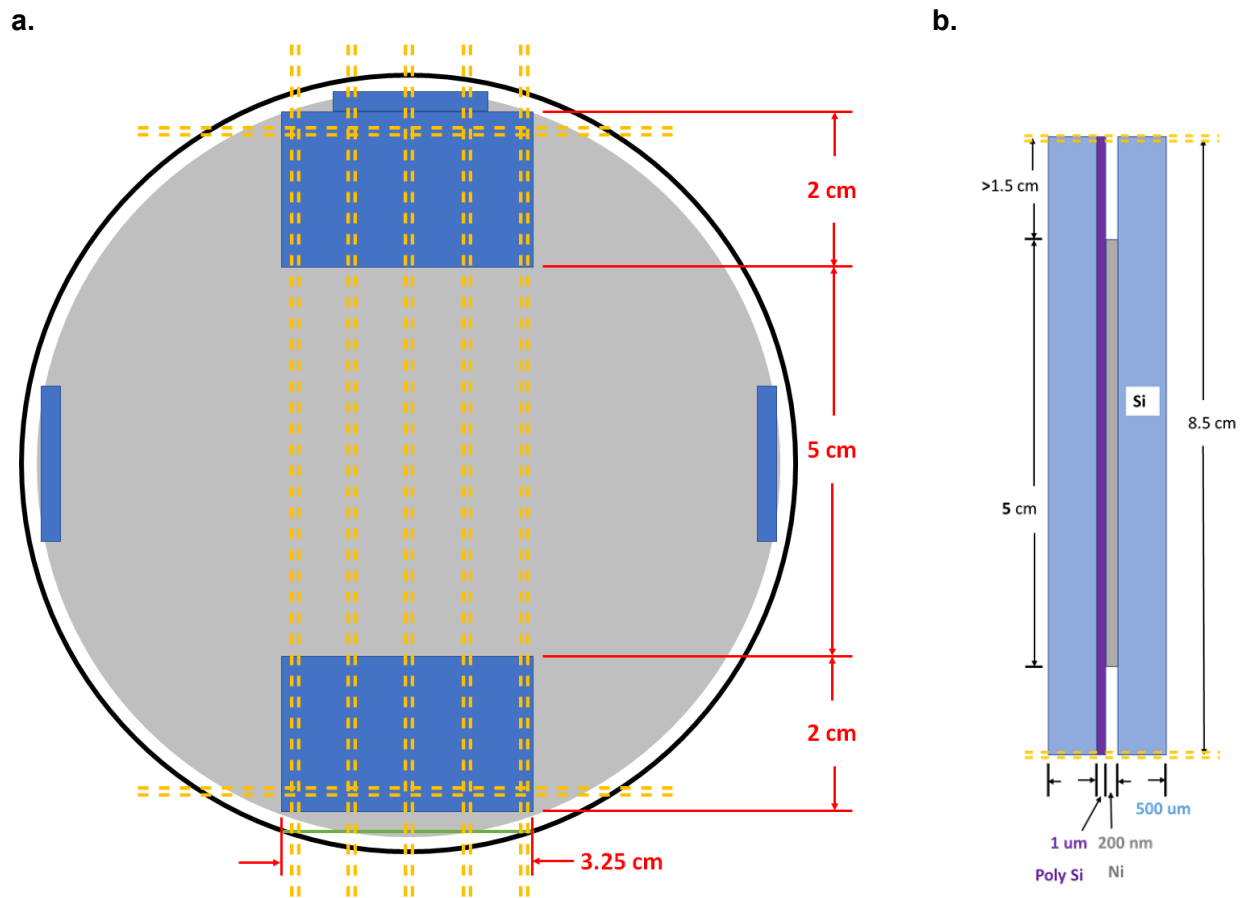


Figure 8: (a) Pattern for DCB testing specimens; blue areas are exposed to be non-metallized after liftoff and yellow hash lines are the dicing cuts. (b) Cross-section of beam specimens.

The beam specimens were tested by the Reinhold Dauskardt lab in the Materials Science and Engineering Department at Stanford University, using a DTS delaminator pictured in Appendix B. Tabs were epoxied onto both sides of an end of the beam at 95°C for 20 minutes, so no



additional annealing effect is expected. The beam was pulled apart at a rate of 1.5  $\mu\text{m}/\text{sec}$  at the beginning of the test until the crack initiated, immediately after which it was compressed at 10  $\mu\text{m}$  per second for about 1 mm. Following crack initiation, the sample was put through alternating stages of tension at 2  $\mu\text{m}/\text{sec}$  and compression at 10  $\mu\text{m}/\text{sec}$  to further grow the crack until final failure. The slope of relaxation and crack propagation determines the fracture energy in the beam and presumably of the bond, depending on what part of the beam the crack propagates through. The crack growth curves for a low temperature and high temperature sample are shown below in Figure 9. The fracture energy is calculated by the equations in appendix B using the slopes of the load/unload stages, with the high temperature bonded sample at 3.67  $\text{J}/\text{m}^2$  and the low temperature sample at 3.56  $\text{J}/\text{m}^2$ .

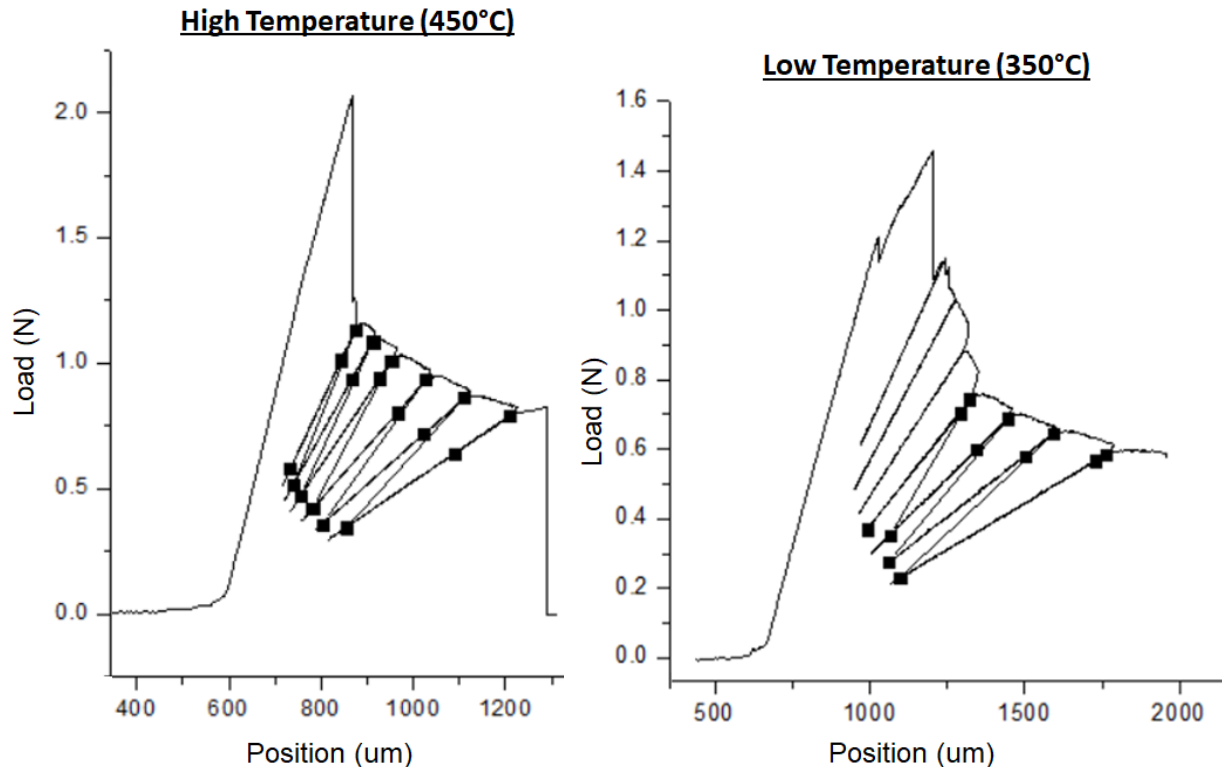


Figure 9: Double Cantilever beam tests - fracture energy  $G_c$  is calculated using the slope of the loading/unloading process.

These are very similar values for samples with different appearances post-delamination, and consultation with Dr. Dauskardt has indicated that this is an extremely low fracture energy. Metal joints usually have values in the range of 100-1000  $\text{J}/\text{m}^2$ . This probably indicates that the crack propagated through the silicon itself or along a brittle interface. The change in slopes in the low temperature sample indicates that the crack propagation changes abruptly during the test, if there is uneven or incomplete bonding. Therefore, the last 3 load/unload curves are used to arrive at the delamination energy.

The delaminated beams were examined with the Sensofar S-Neox optical profilometry tool to determine where the bond failed during the double cantilever beam tensile test. The results for the high temperature sample are shown below in Figures 10 and 11.

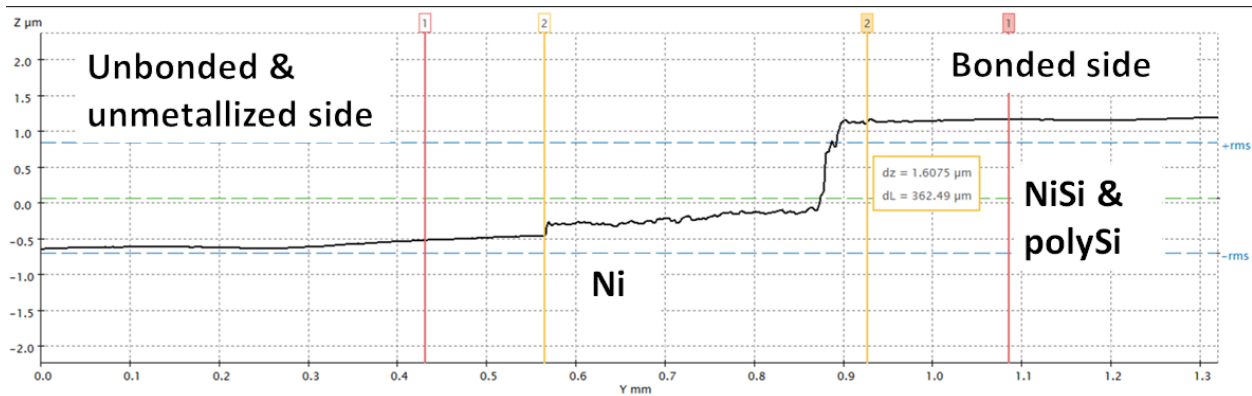


Figure 10: High temperature specimen - Nickel coated base. The ~200 nm Ni and/or NiSi layer is visible before the crack propagates through the polySi layer.

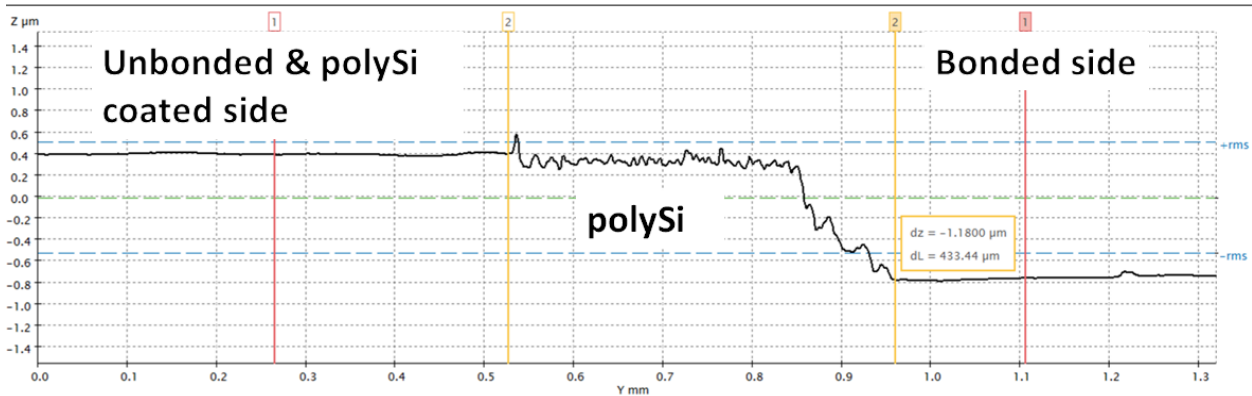


Figure 11: High temperature specimen - PolySi coated wafer.

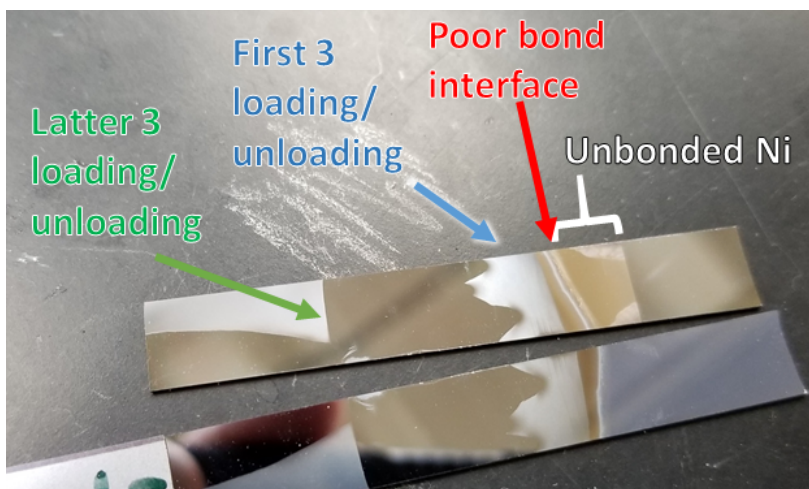


Figure 12: Low temperature specimens. Poor bonding can be observed in the unbonded Ni and in the multiple areas of delamination.

From the profilometry scans of the 450°C sample, the crack propagated through the Ni and NiSi layer for about 300 μm until finally breaking through the polySi side and quickly delaminating the interface between the polySi deposited layer and single crystal Si wafer. While

this result may be surprising at first glance, it is entirely plausible, since we did not strip the native oxide on the silicon wafer prior to doing the polysilicon LPCVD, likely resulting in a weaker-than-expected interface between the silicon and polysilicon. In the low temperature sample, however, the crack behavior is more difficult to decipher. In the general picture of Figure 12, it is shown that there was incomplete bonding and multiple areas of delamination compared to the high temperature bond which was simply a sharp line of delamination a few microns wide. The profilometry images of the bottom beam low temperature specimen shown below depicts the first bond area with the poor partial bonding lines and the initial crack propagation.

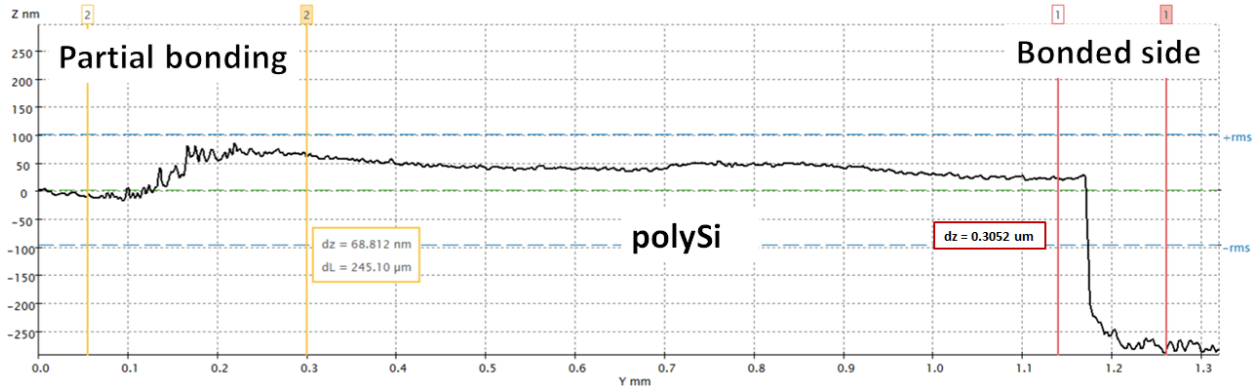


Figure 13: Low temperature specimen - PolySi coated side - first crack propagation interface. Again, after crack propagation through the NiSi interface the polySi splits away from the Si wafer at its interface.

The first striations near the unbonded end of the delaminated sample correspond to rough and uneven areas on the surface of only about 60-80 nm removed (or remaining), which most likely indicates incomplete NiSi formation considering the relatively flat area before the next features. Farther back into the beam corresponding to the visibly gray areas, rough areas with elevated changes between 0.3 -0.4  $\mu\text{m}$  from the flats can be observed. While not as deep as the deposited polySi layer, it is the same side that separates from the Si wafer as in the high temperature sample. The third interface, again visibly grey on the separated beam, is shown in Figure 12 and features the crack propagating through the polySi - NiSi region about 0.9-1  $\mu\text{m}$  deep.

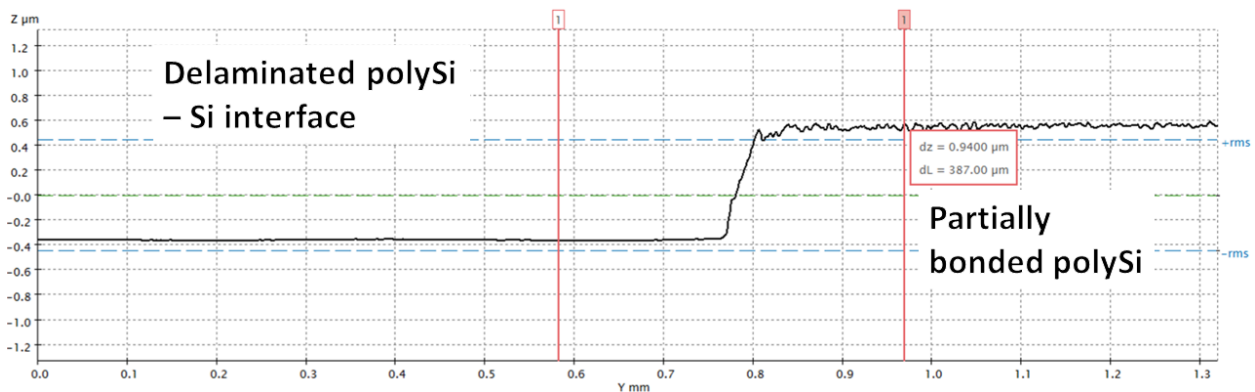


Figure 14: Low temperature specimen - PolySi coated side - second crack propagation interface. PolySi has presumably delaminated from the Si wafer in between crack interfaces, and then the crack propagates 0.9-1  $\mu\text{m}$  deep into the polySi layer.

The crack appears to propagate through the the NiSi-polySi interface rather than the Ni-NiSi layer in the high temperature specimen, based on the rough area being less than 1.0  $\mu\text{m}$  away from the flat single crystal Si wafer.

Considering the unbonded section of Ni and the multiple rough crack delamination sections, the NiSi bond is incomplete and therefore potentially an unreliable bond at the 350°C temperature. At 450°C, the NiSi formation appears to be complete and is apparently strong enough that the polySi layer will completely separate from the Si wafer before a catastrophic failure in the NiSi bond. The NiSi bond is apparently brittle compared to typical metal joints, which may indicate that it could fail under thermal cycling or fatigue situations.

### **Attempted (failed) cobalt silicide bonding**

We attempted to bond a single almost-full coverage cobalt-coated wafer with a polysilicon-coated wafer. The cobalt film was deposited with the Lesker sputterer and was patterned by liftoff. Between deposition and bonding, the cobalt film turned from silver to a brownish color, either due to oxidation or due to a reaction with the liftoff chemicals acetone or Remover 1165. Because we could not find a suitable chemical clean for stripping cobalt oxide or carbonate from the cobalt in literature, only the polysilicon-coated wafer was chemically cleaned before bonding (HF dip as described above). We bonded the wafer at 3340N and 475°C for 40 minutes. Although the wafers appeared to stick together after bonding, they separated catastrophically during the dicing process, with none of the resulting pieces sticking together. The separated pieces showed no sign of bonding.

### **Useful (but orthogonal) notes about fabrication**

Nickel evaporation in AJA:

The crystal monitor program in AJA for monitoring the deposition rate of Ni may be incorrect. We specified a target thickness of 200 nm for the evaporated Ni films in AJA. However, optical profilometry of steps in the evaporated Ni patterns indicate that the actual deposited film has a thickness of about 150 nm. Because this same discrepancy occurred both for films evaporated at a 1  $\text{\AA}/\text{s}$  deposition rate and for films evaporated at a 0.5  $\text{\AA}/\text{s}$  deposition rate, we suspect that crystal monitor may need to be recalibrated for Ni.

Thick (150+ nm) Ni films evaporated onto photoresist in preparation for liftoff suffered from stress peeling when using the 1  $\text{\AA}/\text{s}$  high deposition rate recipe in the AJA. Some photoresist regions curled up and flaked off the wafer while in the tool. Since the silicon regions corresponding to the peeled resist were not metallized, we suspect that the resist peeling and flaking occurs after the deposition, either when the wafers are being transferred from the deposition chamber to the load lock or while venting the load lock. We did not observe any problems when further processing these wafers.

After discussing with staff Mahnaz, Carsen, and Xiaoqing, as well as other AJA users (Paul Comita, Ludwig Galambos), we made the following changes to our process to eliminate stress peeling: (1) baking our wafers at 90°C on a hot plate for 1 minute before evaporation, (2) evaporating a thicker 10 nm Ti adhesion layer, and (3) reducing the Ni deposition rate from 1  $\text{\AA}/\text{s}$  down to 0.5  $\text{\AA}/\text{s}$ . After implementing these changes, we did not experience further issues with resist peeling or flaking during evaporation.

Liftoff:

We attempted to perform Ni liftoff on our first batch of metallized wafers in acetone with ultrasound agitation. While ultrasound greatly accelerated the liftoff process, it produced many large particulates that adhered to the Ni bonding rings. The particles were visible both under the microscope and with the naked eye. S-neox profilometry scans showed that these particles

were at least as tall (200+ nm) as the patterned metal rings, making them unsuitably rough for bonding. For the remainder of the project, we performed liftoff by soaking metallized wafers for 3+ hours in acetone without agitation, which greatly reduced the number of particles on the wafers. Therefore, when preparing metallized wafers for wafer bonding, we suggest doing liftoff by leaving the wafers in acetone for several hours.

Disco:

It is a good idea to only dice wafers that are reasonably well bonded. If the wafers are poorly bonded, there is a tendency for pieces from the top wafer to separate while dicing and get in the way of the blade, increasing the probability of damaging the blade.

Evbond:

The wiki claims that the evbond has a maximum temperature of 500°C. In practice, the tool has difficulty reaching this temperature. For our attempt bonding cobalt to polysilicon, the top and bottom chucks of the tool were set to 475°C. Although the tool was allowed to heat for more than three hours, we could not achieve 475°C at the top chuck (the temperature settled at about 461C), and therefore had to perform the bond at a lower temperature.

## Conclusions and Future Work

In conclusion, we have developed and characterized a nickel silicide wafer bonding process in SNF using the *evbond*. Our characterization of the bonds under different bonding conditions reveal trends in bonding quality as a function of chemical cleaning, bonding temperature, force, and bonding area. Chemical cleaning of both bonding surfaces, especially stripping the native oxide from the polysilicon with HF, is critical to forming a bond. Wafer bonding by nickel silicidation obeys the expected trends for wafer bonding; that is, the bonding quality improves with higher temperature, increased bonding force, and larger bonding surface area. While bonds were successfully formed at temperatures as low as 350°C, bond quality appeared to be best when the bonding process was performed at 450°C. Bond quality does not appear to have any dependence on the bonding pressure, as larger bonding forces tend to produce better results irrespective of the bonding surface area. In addition, double cantilever beam tensile testing accompanied by optical profilometry of the delaminated surfaces quantified mechanical strength of the bond and helped to determine the behavior of the bond upon failure. The NiSi bonding system was determined to produce a wafer-to-wafer bond with delamination energy around 3.6 J/m<sup>2</sup>, corresponding to a brittle and weak bond. In addition, the bonded pair separated catastrophically at the silicon-polysilicon interface rather than at the NiSi interface, a surprising result that may be due to native oxide at the silicon-polysilicon interface.

In the future, the hermeticity and robustness to thermal shock and cycling of the nickel silicide wafer bond should be characterized in order to demonstrate the feasibility of these bonds for vacuum packaging of high temperature MEMS devices. One possible approach to experimentally determining this would be to fabricate vacuum cavities, bond a thin polysilicon lid over the cavity using nickel silicidation in a vacuum ambient, and verify that the bond does not leak by characterizing the deflection of polysilicon lid. The same structures could also be thermally cycled up to operating temperature in an air environment to determine whether seal continues to hold vacuum under thermal stress.

Some additional characterization of the dependence of bond quality on surface roughness and other substrate-dependent parameters may also be needed to determine the feasibility of integrating the nickel silicide bonding process as a step in a full MEMS fabrication flow. The surface roughness for both the polysilicon and nickel surfaces tested in this project are quite low, and the polysilicon wafers are unpatterned and therefore quite flat, corresponding to relatively ideal bonding conditions. Bonding results may differ from those presented here and

may have poorer quality if the bonding surface is not as smooth or flat as the wafers tested in this project.

Electrical characterization and optimization of the nickel silicide wafer bond for high electrical conductivity should be an area for future study, particularly if the bond is to be used as a feedthrough or vertical electrical interconnect.

For the specific application of MEMS thermionic energy converters, the nickel silicide wafer bond also needs to be tested for its compatibility with cesium vapor at operating temperatures. One proposed method for doing this experiment would be to evaporate Ni onto a polysilicon wafer, form the nickel silicide with a thermal anneal, and expose the resulting sample to cesium vapor at high temperatures in a dedicated vacuum chamber setup.

Future researchers may also be interested in characterizing wafer bonding by silicidation with metals other than nickel. The primary criterion for choosing candidate metals is a silicidation temperature low enough that the silicide can be formed in a conventional wafer bonder. Plausible materials systems include platinum silicide (if cost is no object), titanium silicide, and cobalt silicide.

## Acknowledgements

We would like to thank the SNF, Mahnaz Mansourpour, Dr. Xiaoqing Xu, and Uli Thumser for excellent training, Dr. J Provine for guidance on project deliverables and for suggestions on how to characterize our samples, Charmaine Chia for doing SEM, and Yichuan Ding Prof. Reinhold Dauskardt and for DCB testing and analysis. We would also like to thank Dr. Mark Zdeblick, Dr. Mary Tang, and Prof. Roger Howe for advice, feedback, and suggestions.

## References

- [1] Cunningham, S.J., and Kupnik, M. in *MEMS Materials and Processes Handbook*, Ghodssi, R., Lin, P., Eds. (Springer 2011) chap. 11.
- [2] Xiao, Z.-X., *et al.* Low Temperature Silicon Wafer-to-Wafer Bonding with Nickel Silicide. *J. Electrochem. Soc.* 145 (4), 1360-1362. (1998).
- [3] Liu, R., *et al.* High Density Individually Addressable Nanowire Arrays Record Intracellular Activity from Primary Rodent and Human Stem Cell Derived Neurons. *Nano Lett.*, 17, 2757-2764. (2017).
- [4] Dai, X., Nguyen, B.-M., Hwang, Y., Soci, S., Dayeh, S.A. Novel Heterogeneous Integration Technology of III-V Layers and InGaAs FinFETs to Silicon. *Adv. Func. Mat.*, 24, 4420-4426. (2014).
- [5] Philips, W.M. Metal-to-Ceramic Seals for Thermionic Converters: A Literature Survey. NASA Technical Report 32-1420. (1969).
- [6] Weber, E.R. Transition Metals in Silicon. *Journal of Applied Physics*. A30, 1-22. (1982).
- [7] Fernando Novoa. *Adhesion and Reliability of Solar Module Materials*. Ph.D. Dissertation, Stanford University, 2015.
- [8] Perrin Walker, William H. Tarn. *Handbook of Metal Etchants*. Boca Raton, FL: CRC Press LLC, 1991. pp 857-875.

## Appendix A: Detailed process runsheets

### Preparation of polysilicon wafers

1. Clean blank silicon wafers. *Wbclean-res*, 9:1 Sulfuric acid:H<sub>2</sub>O<sub>2</sub>, 120°C for 20 minutes. Dump rinse and SRD.
2. LPCVD 2µm polysilicon layer. *Thermcopoly2*, recipe 620poly, deposition time 1 hour and 55 minutes. Thickness is approximate and likely inaccurate, deposition rate was extrapolated from a shorter deposition on a dummy wafer. Actual measured thickness in SEM around 1-1.5µm.
3. Surface SiO<sub>2</sub> removal, immediately before bonding. *Wbflexcorr1-2*, 1 minute dip in 50:1 HF at room temperature. Dump rinse, blow dry with N<sub>2</sub> gun. Bond immediately after.

### Preparation of patterned evaporated Ni wafers, liftoff with LOL2000<sup>1</sup>

1. Clean blank silicon wafers. *Wbclean-res*, 9:1 Sulfuric acid:H<sub>2</sub>O<sub>2</sub>, 120°C for 20 minutes. Dump rinse and SRD.
2. HMDS singe and vapor prime. *YES*, standard program, 35 minutes
3. Spincoat LOL2000. *Headway2*, 3000 rpm for 1 minute. Use pipette to dispense resist onto wafer as the wafer is spinning at 3000 rpm to make sure wafer is fully covered.
4. Bake wafers. *White-oven*, 1 hour, 180°C
5. Spin-coat 1.6µm SPR3612. *Svgcoat1-2*, no HMDS, 2mm edge bead removal, standard pre-bake
6. Expose. *Heidelberg*, 100 mJ/cm<sup>2</sup>, defocus -2
7. Post-exposure bake. *Svgdev1-2*, bake program 3
8. Develop. *Svgdev1-2*, Standard develop for 1.6µm SPR3612, develop program 4, post-bake program 2
9. Pre-evaporation bake, 90°C for 1 minute on hot plate
10. Evaporate Ti adhesion layer: *AJA-evap*, 10 nm Ti at 0.5 Å/s
11. Evaporate Ni bonding layer: *AJA-evap*, 200 nm Ni at 0.5 Å/s<sup>2 3</sup>
12. Liftoff: acetone soak, *wbflexsolv*, 30min-3hr, carefully rinse off particles in acetone before moving to next solution. Gentle scrubbing with cleanroom q-tip helps to remove metal/resist stringers that persist.
13. Liftoff: Microposit Remover 1165 soak, *wbflexsolv*, overnight (8+ hr) at room temperature, carefully rinse of particles in isopropanol before moving to next solution
14. Liftoff: Isopropanol soak, *wbflexsolv*, 5 minutes, rinse with isopropanol before drying
15. Liftoff: blow dry, *wbflexsolv*, make sure particles are gone before drying.
16. Surface nickel oxide strip, immediately before bonding. *Wbflexcorr1-2*, soak in 5:1 water:29% ammonium hydroxide for 5 minutes at room temperature, dump rinse, blow dry. Bond immediately after.

---

<sup>1</sup> Since our Ni features are large, we did not observe any difference between the wafers patterned with LOL2000 two-layer liftoff vs. regular liftoff. For regular liftoff, omit the YES oven prime step, the LOL2000

<sup>2</sup> Although we specified a 200 nm Ni thickness for the AJA, characterization of our films with *s-neox* suggests that the actual thickness of our layer is about 150 nm.

<sup>3</sup> There is no built-in recipe for evaporating Ni at 0.5 A/s. With permission of staff, we reduced the deposition rate of the 1 A/s recipe down to 0.5 A/s without changing any of the other recipe parameters.



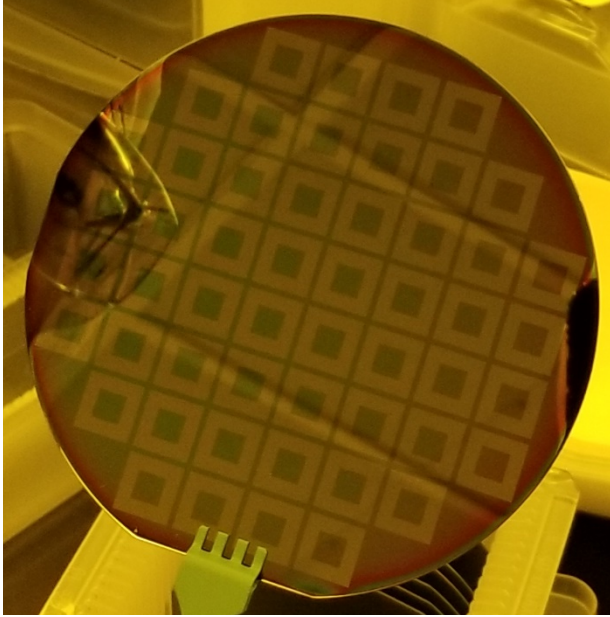


Figure A1: Post-exposure wafer featuring the 50% coverage pattern.

#### Wafer bonding with steel plate in *evbond*

1. Clean wafers with Megasonic cleaner next to the *evbond*. This clean step is useful for removing metal and resist stringers that may have persisted from liftoff.
2. Measure thickness of wafers with micrometers at the *evbond*. Calculate sum total thickness of the wafers, add 3 mm for the graphite plate. Typical thickness 4.150 mm. Set the micrometer on the *evbond* to a thickness greater than this value.
3. Prepare bonding chuck. Stack is: Ni wafer on bottom, flags, polysilicon wafer upside down, quartz plate, solid graphite.
4. Load into *evbond*, make sure flags are in
5. Put in recipe parameters. Relevant parameters are force (in N, 3340N is maximum) and top and bottom temperatures for the chucks (500°C max), and bond time.
6. Run recipe. To save time, we skip the program steps in which the tool waits until it pumps down to 1e-4 millibar pressure. To our knowledge, this does not affect the result. Total run time 3-4 hours, including cooling.
7. Remove wafers from bonding chuck after it has cooled.

#### Dicing

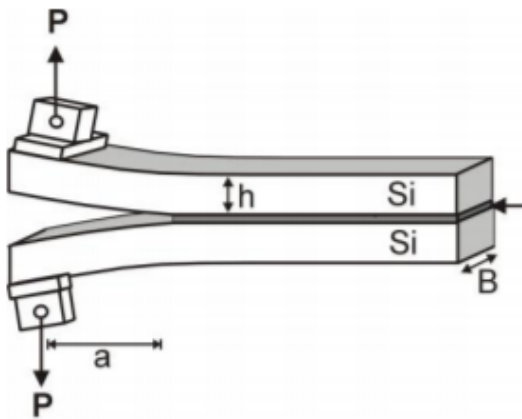
1. Dice wafers into 2cm x 2cm squares. Need special hub blade with 1.62 mm exposure, which is larger than the standard exposure, because the bonded wafer stack is thicker than the exposure for the standard blade.



## Appendix B: DCB Test



Figure B1: DTS Delaminator Machine



$$G = \frac{P^2 dC}{2B da}$$

P: load, C: compliance, a: crack length

$$\frac{\Delta}{2} = \frac{Pa^3}{3EI}$$

$$I = \frac{Bh^3}{12}$$

$$C_{beam} = \frac{\Delta}{P} = \frac{8a^3}{Bh^3E}$$

E: Young's modulus of beam, I: moment of inertia

$$G = \frac{12P^2a^2}{Bh^3E}$$

Figure B2: Delamination illustration [7]

Appendix C: Additional S-Neox images.

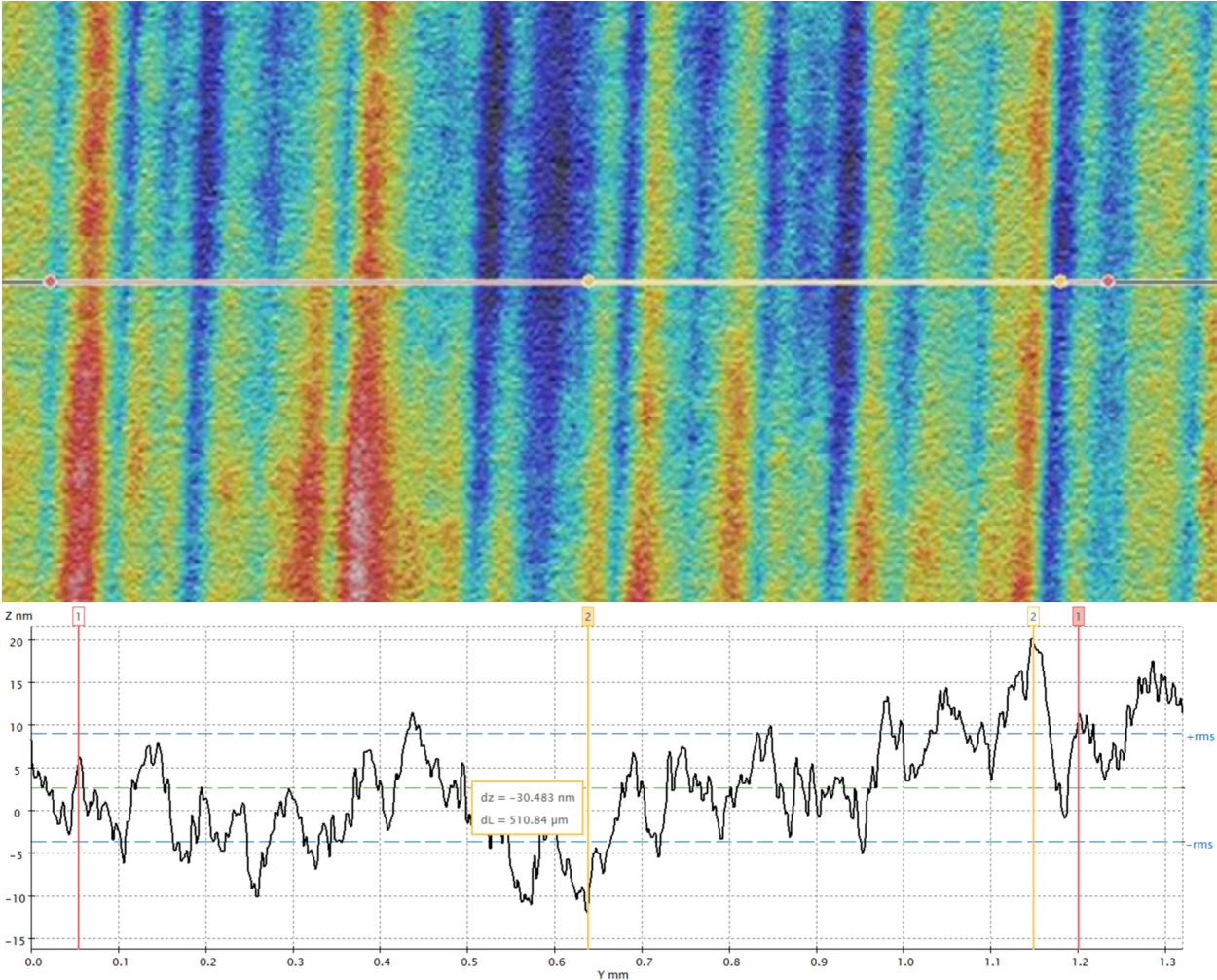


Figure C1: Unpatterned Ni coated wafer in S-Neox. Striations are determined to be an artifact of the profilometry tool trying to read an extremely flat surface with no contrast, as they could be controlled to be lateral or vertical by the user. Measured RMS values are less than 6 nm.

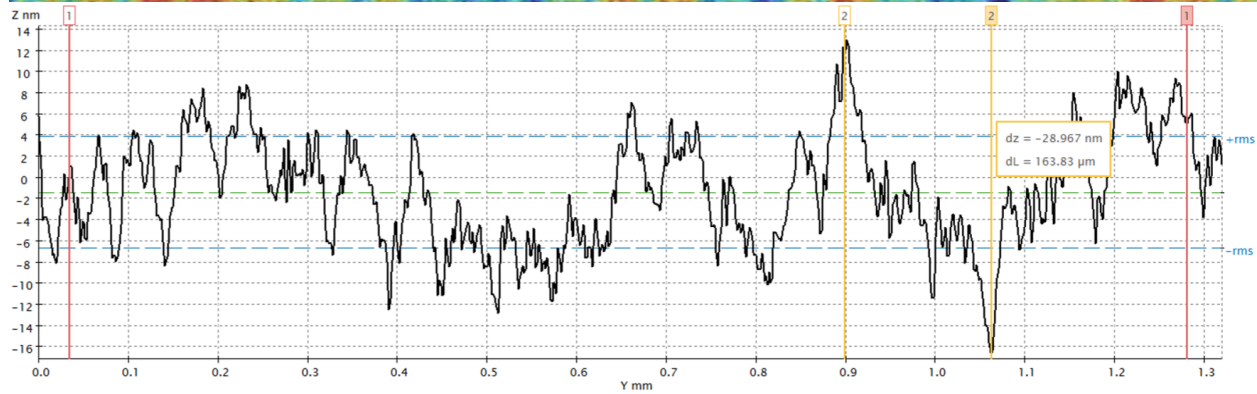
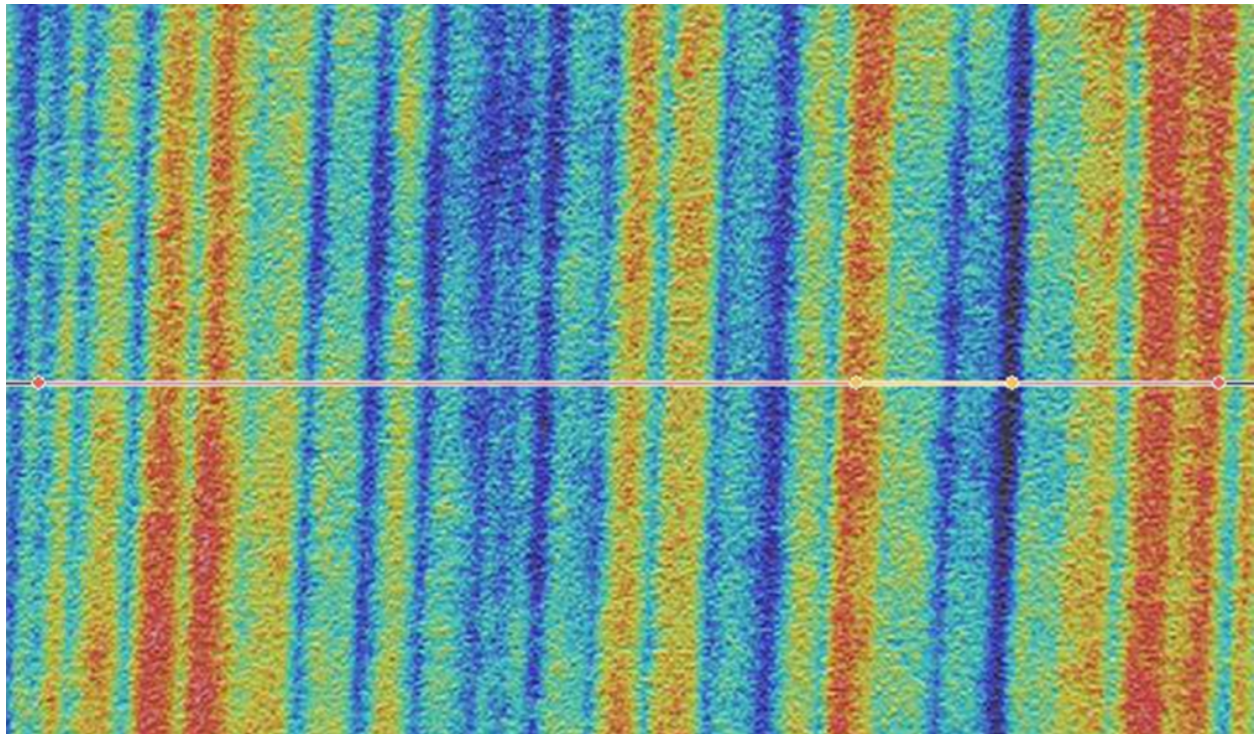


Figure C2: Deposited polysilicon wafer in S-neox. Again, striations were demonstrated to be controllable by the user, and most likely an artifact of the tool's programming. Measured RMS values are less than 4 nm.



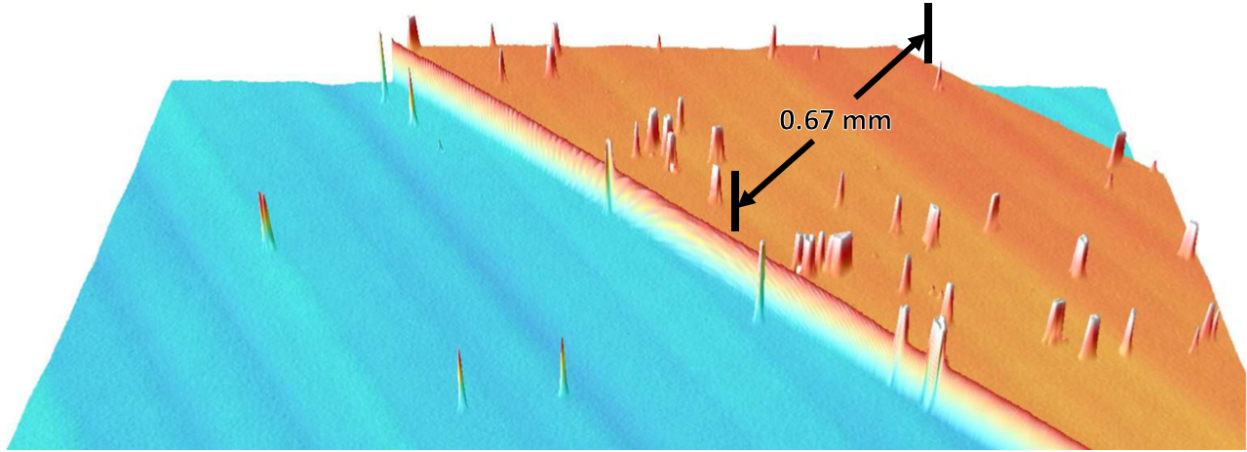


Figure C4: Ultrasonic liftoff - unsuitable for flat surfaces. Tears up metal thin film into tiny pieces that redeposit onto the surface and cannot be removed.

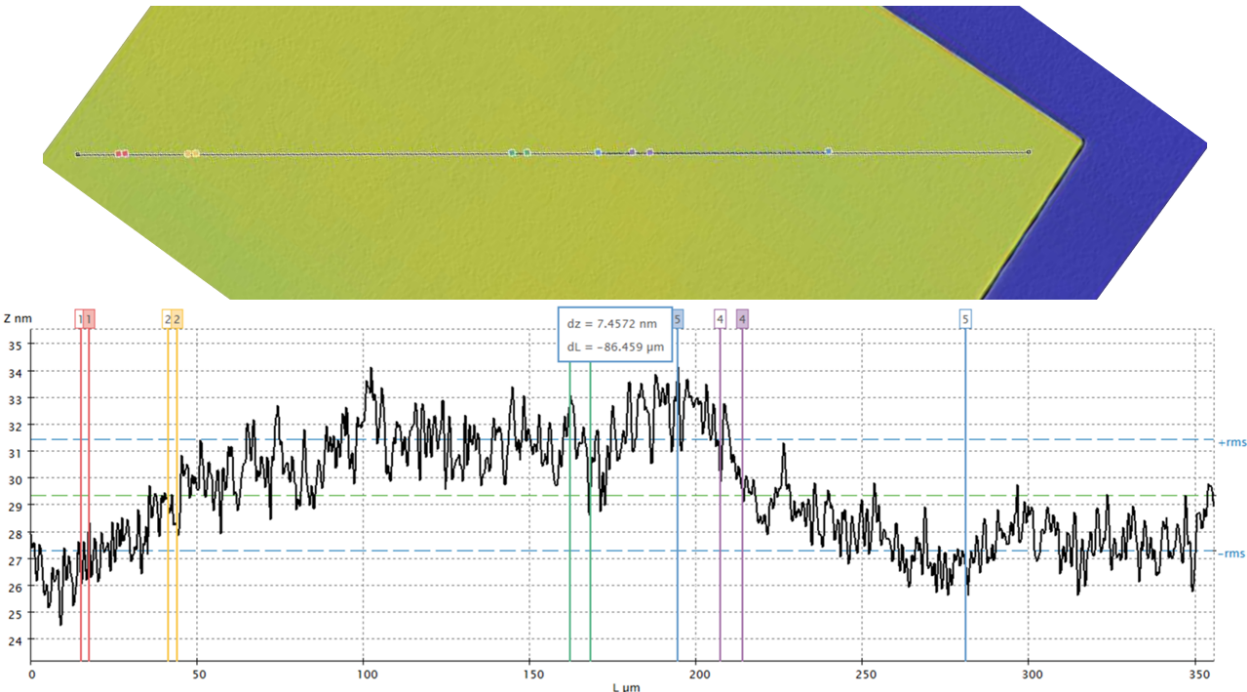


Figure C5: Surface roughness of patterned samples after successful liftoff is about RMS 2 nm. S-neox needs a certain amount of contrast to not produce the striation effect.

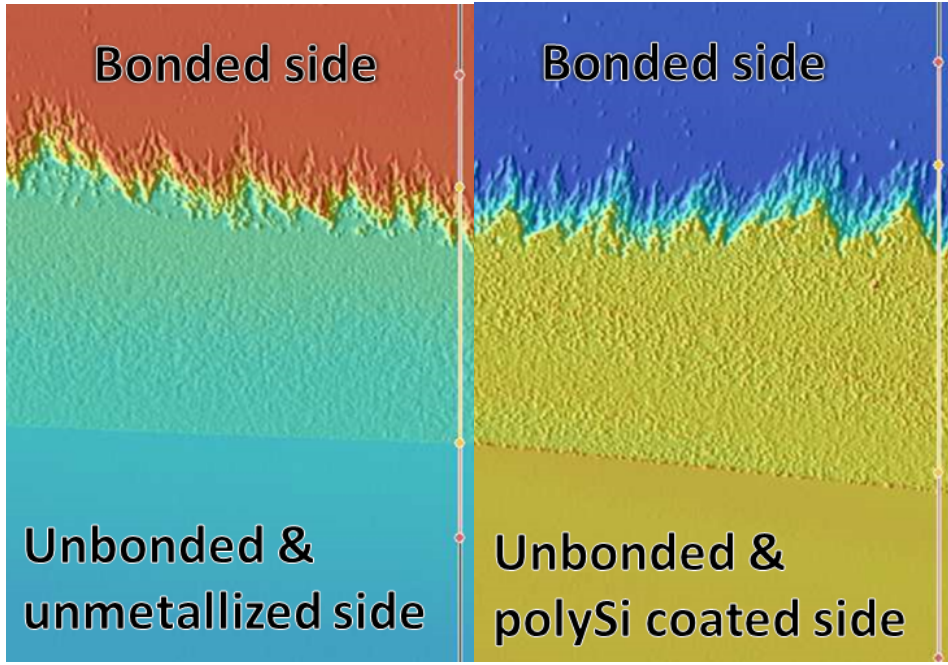


Figure C6: HT - nickel base, 3D

Figure C7: HT - polySi side, 3D

## Appendix D: Full experimental results

Pattern	Ring area	Bond area [m <sup>2</sup> ]	Temp. [C]	Time [min]	Force [N]	Press. [Pa]	Immediately after bonding	Dicing	Razor blade	Bond quality score
10% rings	10%	0.00052	450	40	225	432692.3077	stayed together	stayed together	dies separate cleanly and easily, some transfer of material	1
10% rings, thicker border around edge of wafer	10%	0.00244	450	60	3340	1368852.459	stayed together	stayed together	pieces break rather than separate cleanly, transfer is visible	2
25% rings	25%	0.0013	450		560	430769.2308	half unbonded, unbonded side broke off before sawing	mostly separated	few pieces that survived dicing could not be separated	1
50% rings	50%	0.0026	450	40	1120	430769.2308	stayed together	stayed together	could not separate	2
75% rings	75%	0.0039	450	40	1660	425641.0256	stayed together, dropped wafer, remained bonded		could not separate	2
blanket Ni, no pattern		0.00785 3975	450	40	3340	425262.3671	manually cleaved, pieces remained bonded		could not separate	2
25% rings	25%	0.0013	350	40	560	430769.2308	separated			0
50% rings	50%	0.0026	300	40	1120	430769.2308	separated			0
blanket Ni, no pattern		0.00785 3975	350	40	3340	425262.3671	stayed together, dropped wafer, remained bonded			2
50% rings	50%	0.0026	350	40	1120	430769.2308	stayed together	partially survived	tried three pieces, two	1

								dicing	easily separated except for partial bonded region, third could not separate	
Cobalt, DCB test (mostly no pattern)			475	40	3340		stayed together	Completely separated during dicing, nothing is bonded at all		0
blanket Ni, no pattern, no HF clean		0.00785 3975	450	40	3340	425262.3671	separated			0